Title
Fluorescence lifetime spectroscopy in multiple-scattering environments: an application to biotechnology

Authors
Cerussi, Albert E
Gratton, Enrico
Fantini, Sergio

Publication Date
1999-07-02

DOI
10.1117/12.351028

Fluorescence Lifetime Spectroscopy in Multiple-Scattering Environments: An Application to Biotechnology

A. E. Cerussi, E. Gratton, and S. Fantini
Laboratory for Fluorescence Dynamics, Department of Physics, 1110 W. Green St.
University of Illinois at Urbana-Champaign, Urbana, IL 61801

Keywords: quantitative fluorescence spectroscopy, frequency domain, photon migration, lifetime spectroscopy, bovine mastitis

ABSTRACT

Over the past few years, there has been significant research activity devoted to the application of fluorescence spectroscopy to strongly scattering media, where photons propagate diffusely. Much of this activity focused on fluorescence as a source of contrast enhancement in optical tomography. Our efforts have emphasized the quantitative recovery of fluorescence parameters for spectroscopy. Using a frequency-domain diffusion-based model, we have successfully recovered the lifetime, the absolute quantum yield, the fluorophore concentration, and the emission spectrum of the fluorophore, as well as the absorption and the reduced scattering coefficients at the emission wavelength of the medium in different measurements. In this contribution, we present a sensitive monitor of the binding between ethidium bromide and bovine cells in fresh milk. The spectroscopic contrast was the approximately tenfold increase in the ethidium bromide lifetime upon binding to DNA. The measurement clearly demonstrated that we could quantitatively measure the density of cells in the milk, which is an application vital to the tremendous economic burden of bovine subclinical mastitis detection. Furthermore, we may in principle use the spirit of this technique as a quantitative monitor of the binding of fluorescent drugs inside tissues. This is a first step towards lifetime spectroscopy in tissues.

1. INTRODUCTION

1.1. Uses of Fluorescence Spectroscopy in Turbid Media

Contrast is the key to any spectroscopic or imaging modality. Optical tissue spectroscopy, specifically within the spectral region of 700-900 nm, has enjoyed tremendous success in sensing the concentrations of hemoglobin in both oxygenated and deoxygenated states. The desire to pursue the optical sensing of compounds of physiological interest other than hemoglobin faces the harsh reality of poor contrast. In addition, local environment variables (such as pH) play an important physiological role and are not easily monitored via absorption spectroscopy in tissues. Poor native contrast may be overcome with exogenous contrast agents, particularly those that are fluorescent.

The most notable strengths of fluorescence spectroscopy are highly specific staining (for example, using antibodies) and enhanced sensitivity, especially in the low chromophore concentration regime. There are a variety of emission parameters that depend upon the local environment of the fluorophore. The fluorescence lifetime in particular provides a *quantitative* spectroscopic parameter. Many fluorophores exist that exhibit measurable lifetime changes while either in the presence of physiologically relevant substances such as Ca^{++} and Mg^{++}, or in the midst of variations in local environment conditions such as pH. Research into the fabrication of such fluorophores for *in vivo* use is in progress [1].

1.2. A Similar Problem: A Simple Quantitative Gauge of Bovine Infection

One novel application of fluorescence spectroscopy in turbid media is the determination of the cell density in a milk sample for the purpose of detecting bovine mastitis. The onset of *mastitis*, or the inflammation of the mammary gland, is usually triggered by (but not limited to) pathogenic microorganisms which are typically bacteria. Mastitis has been characterized by two different stages of infection. The full-blown stage, known as *clinical mastitis*, is characterized by visible symptoms such

Part of the SPIE Conference on Time-Resolved Fluorescence Spectroscopy and Imaging in Tissues
San Jose, California • January 1999 • SPIE Vol. 3600 • 0277-786X/99/$10.00

as udder swelling and by systemic symptoms such as fever and appetite loss. Cows infected with clinical mastitis also produce abnormal milk. *Subclinical mastitis,* the precursor stage of clinical mastitis, is much more difficult to detect since there are *no visible symptoms* from the cow or from her milk to suggest infection. The only hints given by subclinical mastitis are decreases in milk production, compositional changes in the milk, and increased numbers of both bacteria and somatic (meaning 'of the body') cells in the milk. For every case of clinical mastitis detected in a herd, there may be between 15 to 40 cases of subclinical mastitis [2].

1.3. Counting Cells Is the Preferred Method to Gauge Subclinical Mastitis

In terms of the ability of a method to predict the infection status on the day of testing, the *somatic cell count* (SCC) has been one of the best [3]. Upon infection, the cow secretes leukocytes (i.e., white blood cells) to combat the invading pathogens. The term somatic refers to all cells in the milk, including leukocytes and epithelial cells. In a strong infection, well over 90% of these somatic cells will be leukocytes (neutrophils, macrophages, and lymphocytes).

Many researchers have found that an increase in the SCC is indicative of udder infections, but it must be stressed that this is not always true in every single case [4]. Although the correlation between the SCC and mastitis is not perfect, the relationship between the SCC and lost milk production follows a general logarithmic pattern. In a large-scale statistical study, Jones *et al.* found that cows with a SCC above 10^5 cells per mL produced less milk and possessed higher infection rates than cows with lower a SCC [5]. Because also they found that this relationship was even stronger for a SCC above 2×10^5 cells per mL, most diary personnel consider 2×10^5 cells per mL to be the maximum SCC for an animal considered free of mastitis.

1.4 Fluorescence Lifetime Spectroscopy as a Means for Determining a Somatic Cell Count

In order to "count" cells with fluorescence we must have a fluorophore that will bind somewhere onto the cell itself. One common cellular target for this purpose is DNA. There is a variety of fluorescent DNA markers but one very common (and inexpensive) one is ethidium bromide. The binding of ethidium bromide to DNA has been the subject of a considerable number of articles [6]. Ethidium bromide binds very tightly to the base pairs of *double stranded* DNA and RNA. In addition, the emission properties of ethidium bromide change considerably upon binding to these base pairs. For example, the fluorescence lifetime of the ethidium bromide-DNA complex is about 12.5 times longer than the fluorescence lifetime of free ethidium bromide in aqueous solution [7]. *Our goal is to use this stark lifetime contrast as a quantitative indicator of the presence of cells inside a turbid medium, in the same way as one would do so in a non-scattering medium.*

1.5. Multiple Scattering Affects Measurements of the Fluorescence Lifetime

The multiple scattering of the medium does, however, change the physics of the problem. Photons propagating inside a multiple-scattering medium undertake a path length that is on average many times longer than the geometrical separation between source and detector. This path length depends upon the optical properties of the medium, unlike the case of the fixed path length of a photon travelling inside a purely absorbing medium. The elongated photon path length complicates measurements of the fluorescence lifetime in both the time- and the frequency-domain approaches by augmenting the time or arrival of a single photon or by increasing the phase shift of the whole collection of detected photons. In cases of photon transport in tissues, photons require a few nanoseconds to traverse a centimeter of tissue, providing a transit time scale comparable with the nanosecond time scale of the fluorescence lifetime. One way to account for the changes in time (phase) from scattering and from fluorescence is the diffusion model of photon transport, which is the subject of the next section. This diffusion-based fluorescence model was first introduced in steady state by Wu *et al.* in 1993 [8]. Patterson and Pogue [9] and Tromberg *et al.* [10] first tested the diffusion model within a frequency-domain approach in 1994. Our model is an extension of this frequency-domain model.

1.6. Why Investigate this Problem?

The first problem of interest entails the development of an inexpensive instrument for determining the SCC of a milk sample. Mastitis is widely regarded as the most costly disease in the U.S. dairy industry and in the entire U.S. animal agriculture a whole [11]. It has been estimated that mastitis costs the U.S. dairy industry $2 billion annually, which amounts to roughly $200 per cow. The economic burden of mastitis is felt the strongest in *reduced milk production.* Bacteria damage the inside of the mammary gland, and eventually lactating tissue is replaced by non-lactating scar tissue. The decrease in milk

production costs the dairy industry an estimated $1.3 billion a year, or 70% of the total estimated loss due to mastitis. Most of these mastitis losses (~ 75%) have been associated with the subclinical as opposed to the clinical stage [12].

In addition, a cell-laced milk sample provides a realistic tissue phantom for the purpose of investigating fluorescence spectroscopy in tissues. To date, there are few fluorophores that possess lifetime contrast mechanisms which have been approved for human testing by the Food and Drug Administration.

2. THEORY

2.1. Notation Conventions

Our chromophores may be divided into two groups. The background chromophores, designated by the subscript *b*, form the first group. In this treatise, we employ the term 'background' to mean anything that is not fluorescent. The *N* independent fluorescent chromophores, designated by the subscript *f*, form the second group. Further, we shall use the subscript *n* as a species index for the fluorophores. Thus, the *total* absorption of the medium takes the form:

$$\mu_{ax} = \mu_{abx} + \sum_{n=1}^{N} \mu_{afx_n} \qquad \mu_{am} = \mu_{abm} + \sum_{n=1}^{N} \mu_{afm_n} \quad . \tag{1}$$

We have also used the subscript conventions of *x* and *m* to denote the excitation and the emission wavelengths, respectively. Thus, μ_{am} represents the absorption of the medium as a whole at the emission wavelength (i.e., λ_m), whereas μ_{afm} represents the absorption of only the fluorescent species *n* at λ_m. The medium also scatters with a strength denoted by the reduced-scattering coefficients μ_{sx}' and μ_{sm}'. We assume that the fluorophores themselves contribute negligible scattering. The fluorescence properties of interest in our case comprise the fluorescence lifetime, τ, the fluorescence quantum yield, Λ, and the fluorophore concentration, which is proportional to μ_{afx} and μ_{afm} through the molar-extinction coefficient, ε, at the appropriate wavelength. Note that τ, Λ, μ_{afx}, and μ_{afm} are all species-dependent quantities.

2.2. Model for Light Propagation: Diffusion Theory

Both emission and excitation photons traveling inside of a highly-scattering medium undergo frequent collisions that give rise to diffusive transport. Diffusion theory, which is a special case of the general formulation of transport theory, has become the standard model used to describe this process [13], [14]. In the frequency-domain approach to diffusion theory, the quantity of interest in the diffusion equation is the *photon density*, $U(r,\omega,t)$ (photons×m^{-3}) where *r* represents the distance between the source and the point in space, *t* denotes the time, and ω represents the angular frequency of the intensity-modulated-light source (i.e., turned on and off at frequency $\omega/(2\pi)$). Our usage of diffusion theory is contingent upon meeting the following approximations (at any wavelength):

(1) We must be at least one transport-mean-free path (~ $\mu_s'^{-1}$) from sources and boundaries.
(2) The media must be scattering dominant (i.e., $\mu_s' >> \mu_a$).
(3) The collision frequency must be much greater than the modulation frequency, or $f << v\mu_s'/(2\pi)$, where *v* is the speed of light in water (cm×s^{-1}).

We shall employ diffusion theory to model the propagation of both excitation and emission light signals.

2.2. Expression for the Excitation Photon Density

The excitation source term is assumed to be an isotropic point source. The solution to the diffusion equation with infinite-medium boundary conditions for an intensity-modulated point source yields the familiar solution of the form $U_x(r,\omega)\exp(-i\omega t)$ (Ref. 15). If we define $P_x(\omega)$ as the source strength (photons×s^{-1}), $\phi_{x0}(\omega)$ as the source phase (degrees), and $vD_x \equiv v(3\mu_{sx}')^{-1}$ as the excitation diffusion coefficient (cm^2×s^{-1}), then $U_x(r,\omega)$ has the form:

$$U_x(r,\omega) = \frac{P_x(\omega)\exp[-i\phi_{x0}(\omega)]}{4\pi v D_x}\frac{1}{r}\exp[-k_x(\omega)\,r] \quad , \tag{2}$$

where $k_x(\omega)$ is the photon-density wave-vector (cm^{-1}):

$$k_x^2(\omega) = \frac{\mu_{ax}}{D_x}\left(1 - \frac{i\omega}{v\mu_{ax}}\right) \quad . \tag{3}$$

2.3. Emission Photon Density

In stark contrast with the excitation point source, the emission source is a *distribution* of point sources dispersed throughout the entire medium. Any fluorophore may become a point source after absorbing an excitation photon. If we add up the photon density waves from all N fluorescent species, and include the detector response, we obtain the *total detected emission photon density* $U_m(r,\omega)\exp(-i\omega t)$, where $U_m(r,\omega)$ is given by [9], [10], [16], [17]:

$$\begin{aligned} U_m(r,\omega) &= \sum_{n=1}^{N} U_{m_n}(r,\omega) \\ &= \frac{P_x(\omega)\exp[-i\phi_{x0}(\omega)]}{4\pi v D_x D_m}\frac{1}{r}\frac{\exp[-k_x(\omega)\,r] - \exp[-k_m(\omega)\,r]}{k_m^2(\omega) - k_x^2(\omega)}\sum_{n=1}^{N}\left(\frac{1+i\omega\tau_n}{1+(\omega\tau_n)^2}\Lambda_n\mu_{afx_n}\Phi_{m_n}\right) \quad . \end{aligned} \tag{4}$$

Equation (4) rests upon a few additional assumptions: (a) there are no interactions between the fluorescent species, (b) photobleaching is negligible, and (c) once an emission photon is absorbed, it cannot be re-emitted (i.e., negligible secondary-fluorescence contribution. Φ_m is defined as the probability that our detector will detect an emission photon from species n (details may be found in [18]). Φ_m depends upon the detector's spectral response, the detector's spectral bandpass, and also the emission probability of species n. The emission optical coefficients now reflect average values taken over the spectral bandpass of the detector.

2.4. Binding Characteristics

If we desire to use Eq. (4) to monitor any binding process, we need a binding model that quantifies the amount of bound and free molecules in the system. One of the simplest models of a reaction is one where the binding sites on the receptor molecule are *independent* of each other (i.e., not cooperative, as in the cooperative case of hemoglobin and oxygen). The mathematical description of such as reaction is :

$$R + G \underset{K_d}{\overset{K_a}{\rightleftharpoons}} C \quad , \tag{5}$$

where R is the number of binding sites (i.e., the receptor molecule), G is the ligand (i.e., the free molecule), and C is the complex (i.e., the bound form of R and G). The association coefficient K_a describes the formation of the complex C:

$$K_a = \frac{[C]}{[R][G]} = \frac{1}{K_d} \quad , \tag{6}$$

where the brackets represent the concentration of the molecule in question. The dissociation constant K_d quantifies the dissociation of C into R and G. The K_d, which is given in units of Molar, tells us that the lower the K_d, the tighter the binding.

Starting with a given number of ligands G_0, the amount of free ligands available will be $G = G_0 - C$ as the complex forms. Similarly, the number of binding sites remaining will be $R = R_0 - C$. Inserting these relationships into Eq. (6) and solving for C results in the following solution in terms of concentration:

$$[C]=\frac{1}{2}\left([R_0]+[G_0]+K_d-\sqrt{([R_0]+[G_0]+K_d)^2-4[R_0][G_0]}\right) . \quad (7)$$

The significance of Eq. (7) lies in that for a given total ligand concentration $[G_0]$, $[C]/[G_0]$ provides the bound fraction of the fluorophore.

3. EXPERIMENT

3.1. Theme of the Measurement: Titration in Cell Density

The principle behind our measurement was to monitor a cell titration in a milk sample using the emission phase as the indicator. We did not know the SCC at the start of the measurement; all we knew at the start of the measurement was that the cow in question was most likely plagued with subclinical mastitis. Given the possibly of an enormous SCC at the start of the measurement, we found it was easier to dilute the number of cells in the sample, while keeping everything else (i.e., the ethidium bromide concentration and the optical properties) constant.

3.2. Instrumentation

The basic components of our standard frequency-domain instrument are presented in Figure 1. The 514.5 nm line of an Ar^+ laser (Stabilite 2017; Spectra Physics, Mountain View, CA) provided the excitation. A Pockels cell provided the intensity modulation (ISS, Urbana, IL). This Pockels cell was biased at 100 V and driven by a radio-frequency sine wave of frequency f that was amplified to an amplitude of about 20 V. The modulated light was collected by a 10X microscope objective and then focused down into a 2 mm core diameter fiber. We took some light away for an optical reference channel by attaching directly a smaller 1 mm core diameter fiber to the side of the larger fiber.

The large-core source fiber was placed inside a 1 L cylindrical beaker. A three-axis positioning device (not shown) moved the source fiber anywhere inside the sample. A 0.6 mm core diameter detector fiber was placed at a distance r away. This fiber was placed well inside the medium so that we simulated an infinite-medium geometry. We used an aspheric lens and a bi-concave lens to collimate the collected light. This collimation was necessary for the interference filters that follow since the throughput of these filters depends heavily upon the angle of the light striking the filter.

When studying the excitation signal, we used an interference bandpass filter centered at 514.5 nm with a 10 nm FWHM (03-Fil-004-514.5; Melles Griot, Irvine, CA). When studying the emission signal, we used a combination of two filters: an interference bandpass filter centered at 600 nm with a 10 nm FWHM (P10-600-F; Corion, Holliston, MA), plus one standard glass longpass filter. The total transmission of this filter combination was approximately 40% at 600 nm, and provided at least 6 OD rejection at 514.5 nm.

The collected light was then focused onto a photomultiplier tube (PMT). This sample channel PMT was driven by another amplified synthesizer signal, this time at a frequency of f+0.00125 MHz. A heterodyning effect was achieved, which produced a 1250 Hz signal that was digitized, Fourier transformed, and analyzed with a personal computer [19]. A master synthesizer provided both a 2 MHz clock signal for the data-acquisition card, and a 10 MHz reference signal to phase lock the synthesizers with the data acquisition card. The software for the card performed the averaging and the fast Fourier transform of the data, which provided the average intensity (DC), the amplitude (AC), and the phase relative to the source.

3.3. The Sample

The major element of the sample was a 1 L volume of fresh bovine milk, which had been taken from a cow who had displayed signs of subclinical mastitis. A testing facility later reported that the milk contained 2.263×10^6 cells per mL. We made certain to complete all measurements with the milk within 24 hours after milking. Throughout the measurement, we verified that the milk was at room temperature. Although we did not measure the pH of the milk, the pH of healthy and infected milk (pH ~ 6.5) does not alter noticeably the binding characteristics of ethidium bromide. In order to label the cells, we added ethidium bromide to the milk to a final concentration of 19.4 μM. Since ethidium bromide cannot traverse the cell membrane, we also added the detergent Triton-X to the sample (0.002 % of the total volume). The pertinent spectroscopic properties of ethidium bromide are listed in Table I [20], [21].

We diluted the milk in order to change the SCC. However, this dilution also lowered in linear fashion the scattering and the absorption optical coefficients of the milk. In order to keep everything of importance constant, we replaced the milk we removed from the sample with an equivalent amount of a Liposyn suspension (20% solids, Abbott Laboratories, Chicago, IL). The Liposyn suspension possessed optical coefficients within about 10 % of the optical coefficients of the milk at λ_x. In addition, both ethidium bromide and Triton-X concentrations in the Liposyn suspension were the same as those in the milk sample. Thus, by replacing milk with this Liposyn suspension, we could keep essentially everything of importance constant, while decreasing the number of cells per mL.

We could not help but notice the interesting colors of milk and Liposyn when laced with ethidium bromide. Without ethidium bromide, both are, of course, white. Upon the addition of ethidium bromide, the Liposyn suspension turned a light pinkish-red color (sort of the color of strawberry milk). This we expected, since the dye remains in solution in the Liposyn, and as such the emission is centered at about 620 nm. However, in the milk the same concentration of ethidium bromide produced an orange hue. This is possible only if DNA is present, since the peak emission for the bound form of ethidium bromide is closer to 600 nm, and hence more orange in color.

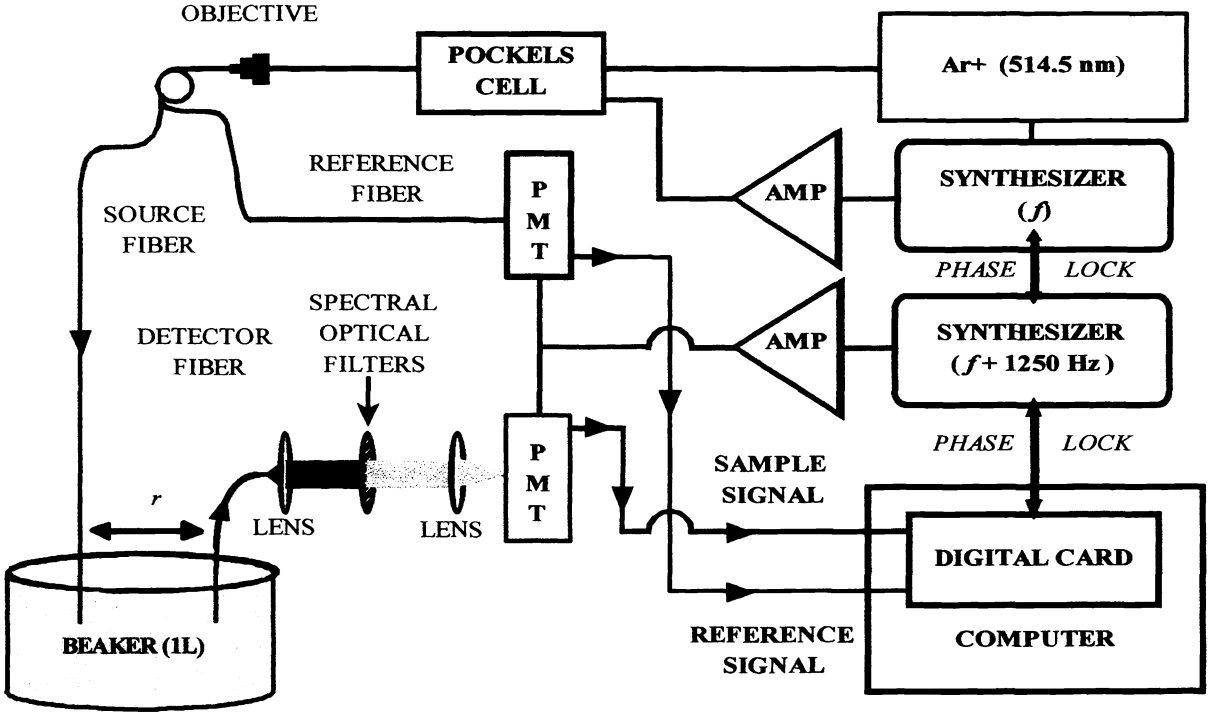

Figure 1 – *Experimental Apparatus.* An Ar^+ laser beam, modulated by a Pockels Cell Modulator, provided a 514.5 nm beam that was focused into a bifurcated optical fiber by an optical objective. One leg of this fiber directed light to a reference photomultiplier tube (PMT) to correct for laser drifts. The other leg of the bifurcated fiber (the source fiber) injected light into the sample medium. Another fiber (the sample fiber) collected light from inside the medium. Both source and sample fibers were placed inside the 1 L sample volume to form an infinite-medium geometry. Although not shown, the sample fiber was moved by a computer-controlled 3D positioning device. The sample fiber sent the collected light to a collection of lenses to collimate the light before passing through optical interference filters. The light was then focused onto a sample PMT. Both PMT's were driven by an amplified (AMP) synthesizer signal. The sample and reference signals were independently cross-correlated down to 1250 Hz, and sent to a data-acquisition card inside a 486 PC computer. The card converted the current to a voltage and then digitized it. Software recorded the sample and reference *DC* intensities, *AC* sample intensity, and the phase. All components of this instrument were phase locked, as indicated by the dotted lines in the figure. Also not shown is the magnetic mixing plate.

3.4. Experimental Protocol

At each cell concentration, we measured the excitation photon density (514.5 nm) at both 10 and 100 MHz, as well as the emission photon density (600 nm) at 10 MHz. We performed the measurement at 100 MHz in order to measure the optical properties of the medium using a multi-distance protocol as described by Fantini *et al.*[22] The excitation measurement served as a reference for the phase in order to determine $\phi_{x0}(\omega)$; in other words, instead of using a reference fluorophore to determine the instrumental phase, as is commonly done in frequency-domain lifetime spectroscopy, we referenced the phase against the scattering of the medium. Starting with the pure milk-dye sample, we diluted the sample in steps of 2 by removing half of the milk-dye sample, and replacing it with an equal amount of the Liposyn-dye suspension. We performed this dilution 10 times, which gave us dilutions ranging from 2^0 to 2^{10} (or 1024). The sample was mixed using a magnetic stir plate, and we were careful to thoroughly mix the sample after each cell dilution. Although the optical properties changed slightly with each dilution, these discrepancies manifest themselves weakly in the emission phase at 10 MHz. Because of the changes in the optical coefficients, we used the average optical properties of all the measurements in the subsequent analysis; this is the reason for the rather large errors in the reduced-scattering coefficients of Table II. We also measured the optical properties at 635 nm with a laser diode in order to estimate the optical properties at 600 nm.

Table I - *Spectroscopic Data for Ethidium Bromide in Free and DNA-Bound Forms*

PARAMETER	FREE	BOUND
absorption peak (nm)	480	518
emission peak (nm)	620	605
ε @ absorption peak (10^3 $M^{-1}\times cm^{-1}$)	5.6	5.6
ε @ 514.5 nm (10^3 $M^{-1}\times cm^{-1}$)	3.53	5.2
ε @ 600 nm (10^3 $M^{-1}\times cm^{-1}$)	~ 0.01	~ 0.05
fluorescence quantum yield (%)	~ 8	~ 100
fluorescence lifetime (ns)	1.73 ±0.01	22 ± 2

4. EXPERIMENTAL RESULTS

Figure 2 presents the changes in the emission phase at 10 MHz resulting from the SCC titration measured at $r = 0.5$ cm. The points represent the measured emission phase from the sample, which we corrected for the autofluorescence of the milk and the Liposyn. The solid line is a prediction of the emission phase, using the optical coefficients given in Table II. Note that in the high SCC range, the phase is essentially constant, which led us to believe that this represented cell densities where the bulk of the ethidium bromide was in a bound state. The fit we performed was one so-called "by eye." The values we used in the fit are listed in Table III.

Table II - *Measured and Extrapolated Optical Coefficients of the Sample*

PARAMETER	EXCITATION	EMISSION
reduced scattering (cm^{-1})	30 ± 2	19 ± 2
background absorption (cm^{-1})	0.0538 ± 0.0006	0.025 ± 0.005

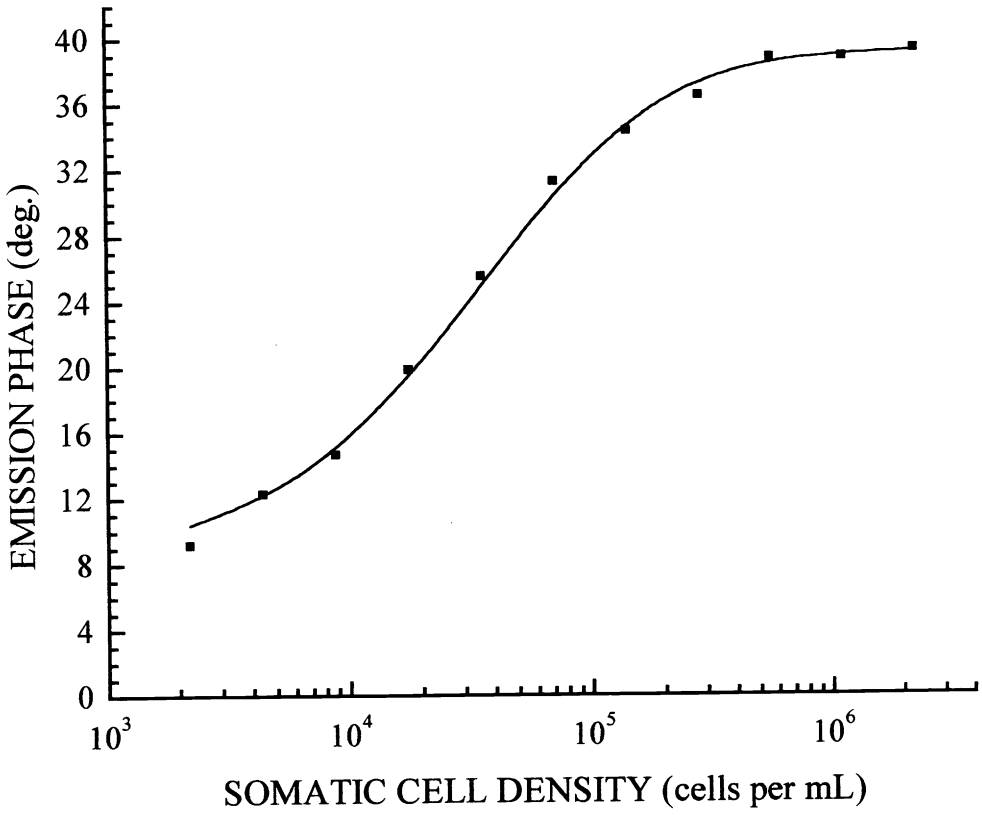

Figure 2 - – *Response of the emission phase to a titration in the SCC.* The points represent the measured phase and the line represents the prediction of the fluorescence-diffusion model. We used Eq. (7) to calculate the concentrations of the bound and free ethidium bromide populations in the sample. The solid line is a best "fit by eye," using the values given in Table **III** and the optical coefficients of Table **II**. The errors in phase are confined within the physical dimensions of the symbols.

Table III – *Fitted Parameters in Figure 2*

PARAMETER	FITTED VALUE
effective K_d (μM)	7.0
binding sites per cell (# per mL)	50×10^9
bound-state lifetime (ns)	12.2
ratio of free-to-bound quantum yield	0.14

5. DISCUSSION

5.1. Discussion of the Fitted Parameters

Although in some ways it is impossible to determine the actual values, each of the fitting parameters actually makes sense if we consider the work of So *et al.* [23]. The additional binding sites provided by the cellular organelles should *decrease* the *effective* K_a, since it is less likely for the ethidium bromide to bind to the cellular organelles than to the DNA. This of course, would *increase the effective* K_d. We are using the term 'effective' to imply the overall binding of the ethidium bromide to any target within the cell. In a pure DNA environment, we would normally expect less than 20 % of the 7×10^9 binding sites per bovine cell to provide targets for ethidium bromide [24], [25]. However, we also would expect that the number of binding sites will also *increase* from the estimate of 10^9 per cell since the ethidium bromide will bind to many targets other than DNA inside the cell. Finally, there is the shortened lifetime. We have observed in other experiments that the bound state lifetime of ethidium bromide in yeast cells is quite a bit lower than it is for DNA in solution. So *et al.* observed in mouse fibroblast cells that ethidium bromide bound to the cytoplasm, the nucleus, and the nucleoli [23]. All of these additional binding sites *lowered* the average lifetime of the bound ethidium bromide. The average lifetime of all of the bound ethidium bromide turned out to be about 12 ns, which is what we measured in Figure 2. Consequently, the ratio of the quantum yields of the free to the bound states must now be about $1.7/12.2 \approx 0.14$ instead of $1.7/22 \approx 0.08$. Factors such as the slight changes in the optical coefficients from dilution to dilution have a miniscule effect on this problem since the photon-density wave at 10 MHz is insensitive to changes in the scattering and in the absorption.

One final note about this plot is in order. There is some interplay between the number of binding sites and the effective K_d. However, lowering the effective K_d below 0.7 μM provided no realistic means to compensate with the number of cells. Physically speaking, we expected the effective K_d to increase. The value of 7 μM offered the lowest effective K_d together with a reasonable number of binding cites per cell that could reproduce the data. We interpreted this to mean that as far as we could tell, this was the best fit.

5.2. Usefulness in Counting Cells

It is clear that the emission phase in Figure 2 tracked the changes in the cell density from within the multiple-scattering medium. The graph monitored the binding of not only the ethidium bromide to the DNA, but also the binding of the ethidium bromide to other cellular components. The question is, so what?

It would be possible to construct a low-cost instrument capable of detecting the SCC of an undiluted milk sample. It would be relatively simple to translate an emission phase into a SCC once a calibration curve has been acquired (as in Figure 2). Such an instrument would use a much smaller sample size, say at least a factor of 100 smaller than the 1 L sample we used. The main sacrifice we must make in reducing the sample volume is that it will be more difficult to measure the optical coefficients accurately. As we have shown, the effect of the uncertainty of the optical coefficients is minimal in this situation since we are looking at photon-density waves at 10 MHz. The reduced scattering of the milk should change in response to changes in the milk-fat content. The fat content of milk is one of the more important compositional quality factors of interest in the diary industry. A highly reflective sample holder could be used to simulate an infinite medium, and allow measurements of the optical properties.

Such an instrument could have two possible audiences. One would be the current testing facilities that test for milk SCC. Currently, the SCC is determined by electronic cell counters and flow cytometers. However, it might also be possible to bring quantitative cell counting to the farm. Dairy farmers might benefit from being able to perform accurate somatic cell counting in milk samples as often as they see fit. Without an actual completed instrument, it is not clear that such ability will be economically helpful. A distinct advantage would be that it could be performed on individual quarters (i.e., one of the cow's four udders), something which testing facilities do not check. The accuracy of the method would be far superior to the subjective California mastitis test (CMT), which is one of the only mastitis detection machines on a farm. Of course, the CMT is also dirt cheap to perform (~ $20 for enough reagent to test many animals).

Regardless, the key issue for such a farm instrument is undoubtedly cost. The price of such an instrument could be quite low. For example, one could use a $3 LED provided by Hewlett Packard, which outputs an amazing 120 mW across a 35 nm bandwidth centered at 472 nm. The modulation depth of this device at 10 MHz is at least 50%, dropping down to about 20% or so at 100 MHz. Ethidium bromide is very cheap, but also very toxic. It would be very nice to produce a unit that could be used as the milking occurs, but the use of a toxic dye might make this difficult.

5.3. Implications for Tissue Spectroscopy

Such a measurement is also possible in tissues. Of course, ethidium bromide may *not* be used in a patient! The spirit of the measurement provides hope that we could perform similar measurements *in vivo* with a suitable fluorophore. Any lifetime difference between bound and free states would provide a tremendous differentiation between the two states. One of the biggest problems in pharmaceutical research is finding out where in a tissue a drug actually settles. It is one thing to develop an anti-cancer drug that destroys cancer cells in a petri dish; it is another problem altogether to get it to achieve this objective *in vivo*. If the drug itself is fluorescent, or if some fluorescent carrier can bring it to the target, it would be possible to study the binding of the drug to its target *in vivo*. This information, provided by a non-invasive *in vivo* measurement, could prove invaluable to the pharmaceutical industry in trying to observe where their drugs actually travel.

Although the results of the fitting in the previous section reflect an effective binding process of ethidium bromide to the cell, using multiple modulation frequencies would provide a means to select populations of binding sites based upon their fluorescence lifetimes. Each organelle or compound with a distinct lifetime could be extracted via this phase-sensitive filtering scheme. This principle is nothing new; it has been used before in frequency-domain fluorescence spectroscopy in non-scattering media. Regardless, the same strengths of frequency-domain lifetime spectroscopy in the cuvette or on the microscope slide apply to the turbid medium as well.

6. CONCLUSIONS

We have performed successful measurements of a titration in the number of cells by monitoring the binding of ethidium bromide to a conglomerate of cellular targets using the fluorescence lifetime as the contrast mechanism. The novelty of the measurement rested with the fact that we performed this measurement in an undiluted fresh milk sample, which had optical properties that were in the same range as those of soft tissues. We were able to quantitatively keep track of the number of cells within this multiple-scattering medium using a diffusion-based model, demonstrating that fluorescence lifetime spectroscopy may be performed in turbid media as in purely absorbing media.

7. ACKNOWLEDGEMENTS

This work was performed in the Laboratory for Fluorescence Dynamics, and it was supported by the NIH (RR03155 and CA57032) and the University of Illinois. The authors also wish to thank Bob Clegg and Chip Hazlett for their invaluable input about the fluorescence properties of ethidium bromide.

8. REFERENCES & NOTES

1. See for example the chapters listed in "Topics in Fluorescence Spectroscopy, Volume 4: Probe Design and Chemical Sensing," edited by J. R. Lakowicz, (Plenum, NY, 1994).
2. W. N. Philpot and S. C. Nickerson, *Mastitis: Counter Attack*, 3-7 (Babson Brothers, Naperville, IL, 1991).
3. U. Emanuelson, T. Olsson, O. Holmberg, M. Hageltorn, T. Mattila, L. Nelson, and G. Åström, "Comparison of Some Screening Tests for Detecting Mastitis," *J. Dairy Sci.* **70**, 880-887 (1987).
4. P. M. Sears, R. N. González, D. J. Wilson, and H. R. Han, "Procedures for Mastitis Diagnosis and Control," Update on Bovine Mastitis, *Vet. Clin. N. A. Food Anim. Pract.*, K. L. Anderson (ed.), **9(3)**, 445-468 (1993).
5. G. M. Jones, R. E. Pearson, G. A. Clabaugh, and C. W. Heald, "Relationships Between Somatic Cell Counts and Milk Production," *J. Dairy Sci.* **67**, 1823-1831 (1984).
6. See for example the large number of references provided in the Molecular Probes catalogue for ethidium bromide.
7. J. Olmsted III and D. R. Kearns, "Mechanism of Ethidium Bromide Fluorescence Enhancement on Binding to Nucleic Acids," *Biochemistry* **16(16)**, 3647-3654 (1977).
8 J. Wu, M. S. Feld, and R. P. Rava, "Analytical Model for Extracting Intrinsic Fluorescence in Turbid Media," *Appl. Opt.* **32(19)**, 3585-3595 (1993).
9. M. S. Patterson and B. W. Pogue, "Mathematical Model for Time-Resolved and Frequency-Domain Fluorescence Spectroscopy in Biological Tissues," *App. Opt.* **33(10)**, 1963-1974 (1994).

10. B. J. Tromberg, S. Madsen, C. Chapman, L. O. Svaasand, and R. C. Haskell, "Frequency-Domain Photon Migration in Turbid Media," *OSA Proceedings in Advances in Optical Imaging and Photon Migration*, R. R. Alfano (ed.), **21**, 93-95 (Optical Society of America, Washington, DC, 1994).
11. National Mastitis Council, "The Mastitis Problem," *Current Concepts on Bovine Mastitis,* 3rd Edition, 6-11 (1987).
12. T. H. Blosser, "Economic Losses from and the National Research Program on Mastitis in the United States," *J. Dairy Sci.* **62**, 119-127 (1979).
13. J. J. Duderstadt and L. J. Hamilton, *Nuclear Reactor Analysis* (John Wiley & Sons, New York, 1976).
14. M. S. Patterson, B. Chance, and B. C. Wilson, "Time-Resolved Reflectance and Transmittance for the Non-Invasive Measurement of Tissue Optical Properties," *Appl. Opt.* **28**, 2331-2336 (1989).
15. J. B. Fishkin and E. Gratton, "Propagation of Photon-Density Waves in Strongly Scattering Media Containing an Absorbing Semi-Infinite Plane Bounded by a Straight Edge," *J. Opt. Soc. Am. A.* **10**, 127-140 (1993).
16. X. D. Li, M. A. O'Leary, D. A. Boas, B. Chance, and A. G. Yodh, "Fluorescent Diffuse Photon Density Waves in Homogeneous and Heterogeneous Turbid Media: Analytic Solutions and Applications," *Appl. Opt.* **35(19)**, 3746-3758 (1996).
17. A. Cerussi, S. Fantini, and E. Gratton, "Quantitative Fluorescence Spectroscopy in Strongly Scattering Media Containing Multiple Fluorophores," *OSA Trends in Optics and Photonics*, E. M. Sevick-Muraca, J. A. Izatt, and M. N. Ediger (eds.), **22**, 70-75 (Optical Society of America, Washington, DC, 1994).
18. A. E. Cerussi, J. S. Maier, S. Fantini, M. A. Franceschini, W. W. Mantulin, and E. Gratton, "Experimental Verification of a Theory for the Time-Resolved Fluorescence Spectroscopy of Thick Tissues," *Appl. Opt.* **36**, 116-124 (1997).
19. B. Feddersen, D. W. Piston, and E. Gratton, "Digital Parallel Acquisition in Frequency-Domain Fluorimetry," *Rev. Sci. Instr.* **60**, 2929-2936 (1989).
20. Spectroscopic data was provided by the manufacturer (Molecular Probes; Eugene, Oregon).
21. We measured the lifetime free ethidium bromide, and used the ratio of 12.5 provided by Ref. 7.
22. S. Fantini, M. A. Franceschini, J. B. Fishkin, B. Barbieri, and E. Gratton, "Quantitative Determination of the Absorption Spectra of Chromophores in Strongly Scattering Media: a Light-Emitting-Diode Based Technique," *Appl. Opt.* **33(22)**, 5204-5213 (1994).
23. P. T. C. So, T. French, W. M. Yu, K. M. Berland, C. Y. Dong, and E. Gratton, "Time-Resolved Fluorescence Microscopy Using Two-Photon Excitation," *Bioimaging* **3**, 49-63 (1995).
24. The Center for Biological Sequence Analysis at the Technical University of Denmark maintains a website that lists the genome sizes of a variety of organisms. This useful site is called DOGS (Database of Genome Sizes) and it has the address *http://www.cbs.dtu.dk/databases*.
25. M. J. Waring, "Complex Formation between Ethidium Bromide and Nucleic Acids," *J. Mol. Biol.* **13**, 269-282 (1965).